International Journal of Advanced Science and Technology
Vol.67 (2014), pp.43-58
http://dx.doi.org/10.14257/ijast.2014.67.05

Role of Pico Second PEF On Osteoblast Intra organelle Nanoporation

S. Sarkar[1] and R Mahapatra[2]

[1]*Dept of Applied Electronics and Instrumentation, SMIT, Sikkim, India*
[2]*Dept of Electronics Communication Engineering, NIT Durgapur, India*

[1]*swarupsarkar957@yahoo.com*

Abstract

This paper presents the effect of pico pulse electric field on intra organelle nano poration of multi layer osteoblast cell placed in a 3D non uniform microfloudic chip composed of bi metallic heterogeneous micro electrode under the influences of smart control FPGA based pico pulse generator and images of intra organelle nanoporation are recognized by neural fuzzy network. It is observed that When the micro pulse is applied the cell starts to response but it is unable to penetrate the intra cellular nucleus- membrane where as the expected results will come when the Pico pulse is applied on the cell, a number of nana pores are generated on the intra organelle and chemicals are entered into the cell. It is also exposed that the key parameter of nanoporation such as intra organelle voltage, pore radius, pore density, pressure, surface tension and ion uptake are externally controlled by user defined hybrid 3D micro chip and FPGA based pico pulse generator. The application of neural fuzzy network for succesfull reorganization of nanoporative image is completely explore.

Keywords: *Picoseconds Pulsed Electric Field (psPEF), Bi metallic electrode, intrigrated bio Micro chip, Dense Osteoblast cell, Intra- organelle, nanoporation. Neural fuzzy network*

1. Introduction

The typical morphological structure, the osteoblast cell is more rigid than other biological cell. This structure gives a challenge to the scientist for its nanoporation and its intra organelle characterizations. Although some experiment and theoretical approach have been performed on outer membrane but the pore formation in intra organelle concept is till now limited. Previously some work has been done considering the single layer structure of osteoblast cell which gives the limiting information about the cell electroporation. We are focusing on that limitation and consider the original bi-layer structure of osteoblast cell. In our study we observed that the pico pulse has a remarkable response on intra cellular pore generation having the pore radius of $10^{-10}m$ *l*evel if the rigid cell is placed into a specially design micro chip where shape of micro fluidic channel and micro electrode are hybrid in nature and electrodes are bi metallic [1-4].

In our previous study [14-15], proposed a new method to construct 3D hybrid bio micro chip by utilizing low melting point bismuth (Bi) and Au metal alloy. The functionality of 3D electrodes fabricated by this method was demonstrated by particle manipulation and separation [12-13]. This method offers many advantages such as good conductivity, highly efficient, low cost, simple fabrication and time saving, since the process resembles the fabrication method used for planar electrodes, favorable in DEP application due to the large

ISSN: 2005-4238 IJAST

electric field gradient produced by hybrid shaped 3D electrodes and improvement of topological electrode design.

In recent developments of micro technologies and micro fluidics techniques permit consideration of the design and fabrication of new innovative tools for biology. The main benefits of these technologies consist in their miniaturization and parallelization capabilities, as well as real-time observation in the case where transparent materials are used for the device fabrication. But till now the information regarding the effect of Pico pulse on intra cellular organism of dense rigid cell like osteoblast cell are limited. However, the delivery of the psPEF to the cells without deformation of biological contents requires a specific design [5-8]. In this context, the work presented in this paper describes the design, fabrication and characterization of a hybrid micro chip device specifically optimized for ps PEF exposure of intra organelle picoporation of dense osteoblast cell followed by the development of a micro-fluidic model of the system of our current study. Biological characterizations of the cells exposed on the chip to 10 ps pulsed electric fields using a florescent dye are carried out. The effect of pico pulse on intra organelle nanoporation includes the prime importance to provide the new knowledge on drug delivery system and bone cancer treatment.

2. Analytical Study

2.1 Effect of pico pulse on the induced intra organelle voltages

C.Yao *et al.* gave the following Schematic diagram of double -shelled spherical cell in suspension, which is used for theoretical explanation of outer and inner membrane potential of a biological cell [18-19]**.**

According to the transfer functions defined by C.Yao the inner and outer membranes to a given rectangular pulse electric field *E*(*s*) can be obtained

$$V_{org(i)}(t) = L^{-1}[Hn(S).E\ (S)] \text{ ------} \quad (1)$$

$$\& \ V_{org(o)}(t) = L^{-1}[Hm(S).E\ (S)] \quad (2)$$

Where,

$$Hm(\ s\ ) = \frac{Vm(s)\cos\theta}{E\ (\ s\ )} = \frac{1.5Rc\cos\theta}{\tau cll\ S+1}$$

$$\& \ Hn(S) = \frac{Vn(S)\cos\theta}{E(S)} = \frac{1.5\ \tau cell\ Rn\cos\theta}{(\tau nuc\ S+1)+(\tau cell\ S+1)}$$

After simplification of equation (1) & (2) we get

$$V_{org(o)}(t) = 1.5\ Rc\ E\ (t)\left[-e^{\frac{t}{\tau cell}} - 1(t-\tau) + e^{\frac{t-\tau}{\tau cell.}}1(t-\tau)\right]\cos\theta -- (3)$$

$$V_{org(i)}(t) = \frac{1.5\ \tau cell\ Rnuc\ E\ (t)}{\tau cell-\tau nuc}\left[(e^{\frac{t}{\tau cell}} - e^{\frac{t}{\tau nuc}}) - (e^{\frac{t-\tau}{\tau cell}} - e^{\frac{t-\tau}{\tau nuc}}).1.(t-\tau)\right]\cos\theta -- \quad (4)$$

As we know that$E(t) = v/d$, where v=applied voltage & d= distances in between two electrode. We replace $E(t) = v/d$ in equation (3) & (4) and get outer membrane potential is

$$V_{org(o)}(t) = 1.5\ Rc\ \left(\frac{v}{d}\right)\left[-e^{\frac{t}{\tau cell}} - 1(t-\tau) + e^{\frac{t-\tau}{\tau cell.}}1(t-\tau)\right]\cos\theta -- \ (5)$$

& inner membrane is

$$V_{org(i)}(t) = \frac{1.5\,\tau cell\,Rnuc\,(v/d)}{\tau cell-\tau nuc}\left[(e^{\frac{t}{\tau cell}} - e^{\frac{t}{\tau nuc}}) - (e^{\frac{t-\tau}{\tau cell}} - e^{\frac{t-\tau}{\tau nuc}}).1.(t-\tau)\right]\cos\theta \text{ ---- - (6)}$$

As we know that E (t) = v/d, where v=applied voltage & d= distances in between two electrode. We replace $E(t) = v/d$ in equation (5) & (6) and get outer membrane potential $(Vm(t))$ is

$$V_{org(o)}(t) = 1.5\,Rc\,(v/d)\left[-e^{\frac{t}{\tau cell}} - 1(t-\tau) + e^{\frac{t-\tau}{\tau cell.}}\,1(t-\tau)\right]\cos\theta\text{---- (7)}$$

& inner membrane is

$$V_{org(i)}(t) = \frac{1.5\,\tau cell\,Rnuc\,(v/d)}{\tau cell-\tau nuc}\left[(e^{\frac{t}{\tau cell}} - e^{\frac{t}{\tau nuc}}) - (e^{\frac{t-\tau}{\tau cell}} - e^{\frac{t-\tau}{\tau nuc}}).1.(t-\tau)\right]\cos\theta\text{------ (8)}$$

2.2 Effect of pico pulse on the radius of nanopores:

Based on the theory of membrane permeabilization, nano pores are initially created with a radius of r*. By increasing the applied electric field, nano pores start to develop in order to minimize the energy of the cell membrane. For the intra organelle with n nanopores, the rate of change of their radius of pore(r), can be determined by the following set of equations [20]

$$U(r,Vn,Ap) = \frac{D}{KT}\left\{4\beta\left(\frac{r^*}{r}\right)^4\frac{1}{r} - 2\pi\gamma + 2\pi\sigma r + \frac{[\Delta\varphi]^2 Fmax}{1+rh/(r+ri)}\right\}\text{-- (9)}$$

Where D is the diffusion co efficient , K = boltz man constant, T =absolute temp, $\varphi(r,\theta)$ =intra organelle potential. $\gamma = surface\ tention.$ The constants of the above equations are defined in Table 1.

2.3 Effect of pico pulse on the intra organelle pore current

On the other hand from the some references we have come to know that the outer & inner membrane pore current are expressed respectively[21],

$$Iepi = \frac{\pi r m^2 \sigma\Delta\varphi}{Fh} * \frac{e^{(\Delta\varphi-1)}}{\frac{w0 * e^{(w0-nvn(t))} - n\Delta\varphi}{w0-nV(t)} * e^{\Delta\varphi(t)} - X} - (10)$$

$$\text{And } X=\frac{w0*e^{(w0+nvn(t))}+n\Delta\varphi}{w0+nV(t)}\text{. --------- (11)}$$

Where $Iepi$ Intra organelle pore current.

2.4 Effect of pico pulse on the intra organelle pressure:

From various literature surveys, it is come to know that when electric field is applied on a biological cell specific pressure is inserted into the membrane which is mathematically expressed as [21]

$$\&\ Pi = \frac{\varepsilon n\Delta\varphi^2}{2h^2}\text{---------- (12)}$$

2.5 Effect of pico pulse on the intra organelle surface tension

As we know when the electric field is applied on the biological cell its molecular & chemical property are changes which may cause the change of surface tension which is mathematically expressed as [21]

$$\Gamma in = \frac{2*\varepsilon n*\Delta\varphi}{hi} \text{---------- (13)}$$

Where Γin is the surface tension of intra organelle and hi are the thickness of inner membrane.

2.6 Effect of pico pulse on the intra organelle pore density

DeBruin KA, Krassowska W, exposed that the rate of creation of nanopores at intra organelle can be found as [22].

$$\frac{dN(t)}{dt} = \alpha * e^{\left(\Delta\varphi/Vep\right)^2}\left(1 - \frac{N(t)}{Neq(Vn)}\right) - - - - - - (14)$$

Where $N(t)$ is the pore density.

3. Used Parameter

Table 1. Values for constants and parameters used in the simulations.

parameter	Cell parameters	value	
conductivity (S/m)	Extracellular medium (σe)	10×10^{-3}	[20]
	Cell membrane(σm)	1.2×10^{-7}	
	Cell cytoplasm(σc)	0.039s	
	Nuclear membrane(σn)	10×10^{-1}	
	Nuclear cytoplasm(σn)	0.08s	
relative permittivity	Extracellular medium(εe)	80	
	Cell membrane(εm)	22	
	Cell cytoplasm(εc)	93	
	Nuclear membrane(εn)	22	
	Nuclear cytoplasm(εn)	93	
Geometry parameter (μm)	Cell radius(rc)	12 μm	
	Cell membrane thickness(d)	0.006µm	
	Nuclear radius(rn)	6 μm	
Constant parameters	$N0$	$1 * 10^9$	
	D	$5 * 10^{-14}$	
	K	$1.38065 * 10^{-23}$	
	T	300	
	β	$1.4 * 10^{-19}$	

	γ	$1.8 * 10^{-11}$	
	$Fmax$	$0.7 * 10^{-9}$	
	σ	$1 * 10^{-6}$	
	rh	$0.97 * 10^{-9}$	
	ri	$0.31 * 10^{-9}$	
	r	$0.7 * 10^{-9}$	
	r 1	$1.2 * 10^{-9}$	

Table 2. Design consideration of the micro chip

Devices	Parameter	Value	Unit
Chip	Length	2300	μm
	Height	100	μm
	Width	900	μm
	Inlet	10	μm
	Outlet	10	μm
Micro Electrode	Length	1000	μm
	Width	900	μm
	Height	100	μm
	Inter electrode gap		μm
	Central part	50	μm
	Medial part	150	μm
	Lateral part	250	μm
	Material	Au ,Bi	
Micro channel(Bi-lateral)	Length	2300	μm
	Width	250	μm
	Height	100	μm

4. Materials and Methods

4.1 Pico Pulse Exposer system

As it is revels that the pico pulse signal has a an important role for nanopore formation within the intraorganelle or nucleous membrane [16-17] so author gives an extra concentration for the design of pico pulse generator.To obtain the perfect pico signal the author smart control FPGA technology and the following schematic diagram is used for simulation of pico pulse, which is applied to the COMSOL simulated 3D hybride microchip, that provide the best option for intraorganelle nanoporation of rigid osteoblast cell. The simulating pico pulse electric field exposer system is describe bellow.

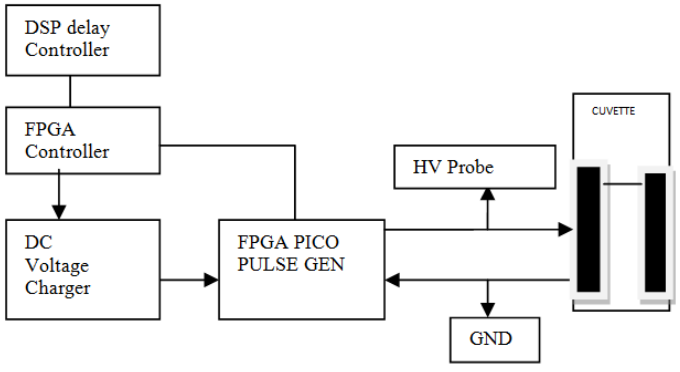

Figure 1. Pico pulse electric field exposure system for nanoporation

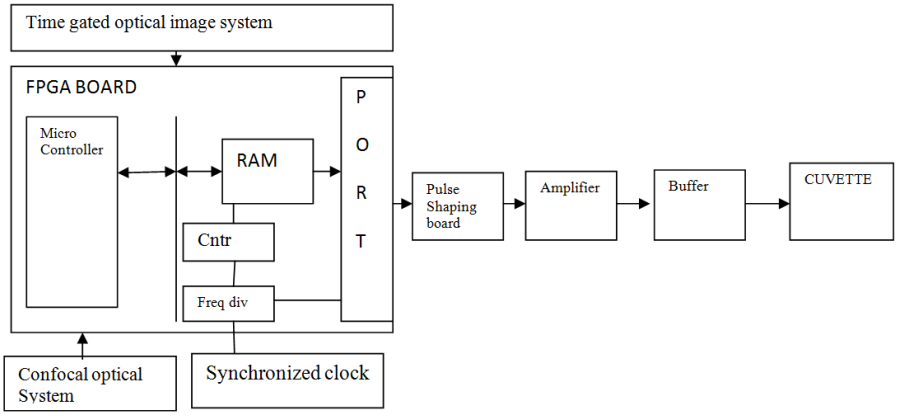

Figure 2. FPGA control pico pulse generator

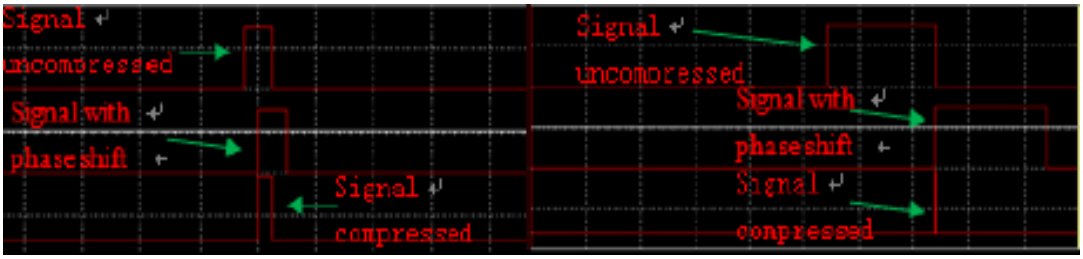

Figure 3. Simulated graph for FPGA control pico pulse generator

The Figure 1 shows the pico pulse electric field exposure system. The exposure set-up is composed of Pico second pulse generator unit, high voltage probe, DSP delay controller, FPGA controller, and FPGA based pico pulse generator which allow delivering the pulses to the biological medium. Pico pulse is generated by embedded FPGA programmable pulse generator which is shown in Figure 2 and it is monitored by FPGA controller and. The pulsing sequence was controlled by a DSP delay controller. The voltage waveform was monitored using a voltage probe. The voltage in the final pulse was slightly reduced due to medium temperature rise. The medium temperature during pulsing was monitored using a fast radiation thermometer (RT) with a response time of 10 ms, sufficiently fast to monitor the overall temperature change during the repetitive pulsing. The applied voltage across the biochip electrodes is measured by a HV probe .The probe has a large frequency bandwidth 6 (GHz) and is designed to have the output terminated into the system with a voltage ratio of 1:10. For the measurements, the two conductor pins of the probe are placed in direct contact with the input or output of the gold bismuth electrodes (in COMSOL simulating devices).The output wave form of pico pulse generator is shown in Figure 3. In this figure the compressed and uncopressed both signels are obtained but in this current doctoral research the uncompressed signal is used.

4.2 Sample Preparations

Mouse calvarias osteoblastic cells were used in this study .In order to observe only the effect of the micro devices on cells; a standard culture medium was used for all experiments. To do so, osteoblastic cells were cultivated in a standard T75 Falcon culture flask

supplemented with penicillin (100 units/ml) and streptomycin (100 mg/ml), 15% fetal calf serum and with neither ascorbic acid nor beta-glycerophosphate and dexamethasone.

4.3 Set up for intrigrated intraorganelle nanoporation system

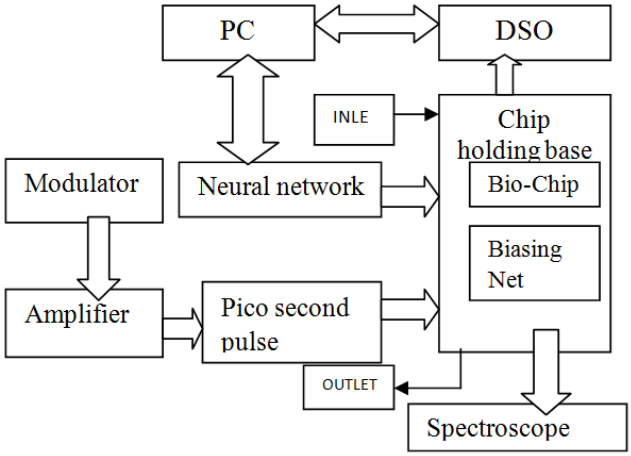

Figure 4. Block diagram of intrigrated intraorganelle nanoporation system

Figure 4 shows the block diagram oh intrigrated intraorganelle nanoporation system which consist of bio chip holding base, pico pulse exposure, neural network, spectroscope and personal computer (PC). The bio chip holding unit used for properly places the micro chip along with input and output syringe pump. The high intense programmable pico pulse exposure provides dedicated suitable pulse to the micro chip. Neural network is used for efficient intra organelle nanoporative image reorganization and output image is exposed through spectroscope and digital storage oscilloscope. The complete set up is control by PC.

4.4 Biological experiments

In our study the experimental biological tests are performed with 20 ps duration pulses. A train of 200 psPEF, square shaped, 20 ps duration is applied with a repetition frequency of 234 Hz. A view (fluorescence or bright field microscopy) of cells within the 3D hybrid micro chip is recorded before and just after the application of psPEF. As shown in Figure 4, Cells fluoresce in red after the application of psPEF, proving that PI introduces into the cytosol, due to the disturbance of the plasma membrane, Note that the observation is made with functional cells located in the white circles drawn on this figure. Viability of cells submitted to psPEF treatment was checked thanks to Trypan Blue test. An average of 90 ± 1% of exposed cells remains still alive 30 min after being exposed to ps PEF. The number of nano pulses that were applied (200 or 300 pulses), to confirm the effect of these parameters on the intra cellular nanoporation. As expected, the number of pulses and their amplitude both influence the level of permeabilization. These preliminary characterizations of the effect of nanoporation on intra organelle, in particular on the permeabilization of the plasma membrane, were permitted thanks to the real time Observation on the miniaturized bio device. Deeper exploitation of this type of device will be conducted together with the development of new psPEF generators.

Actual results demonstrate the capability of the developed 3D hybrid bio micro chip to address the effect of psPEF to the intra organelle nanoporation of multilayer osteoblast cell within the micro chip.

4.5 Experimental Data

Table 3. Percentage of permeabilized cells depending both on the number and amplitude of applied psPEF

Condition		% of permeabilizations
Applied electric field (KV/Cm)	No of pulse	
30	150	58
35	175	60
40	200	72
45	200	85
45	250	87
50	250	90
50	300	95

The above Table 3 shows the percentage of permeabilized cells depending both on the number and amplitude of applied electric field. By the influences of above pulse it is observed that at pico pulse a large amount of dedicated chemicals entered into the intra organelle and all experimental values are explored through the graph bellow.

Table 4. Experimental data

Pulse duration (X-axis) second	Flu recent intensity (Y-axis)no of molecules
10^{-6}	0
10^{-7}	10,000
10^{-8}	15,000
10^{-9}	20,000
10^{-10}	40,000
10^{-11}	80,000
10^{-12}	100,000
10^{-13}	100,000
10^{-14}	100,000

The above experimental values are represented by the graph bellow.

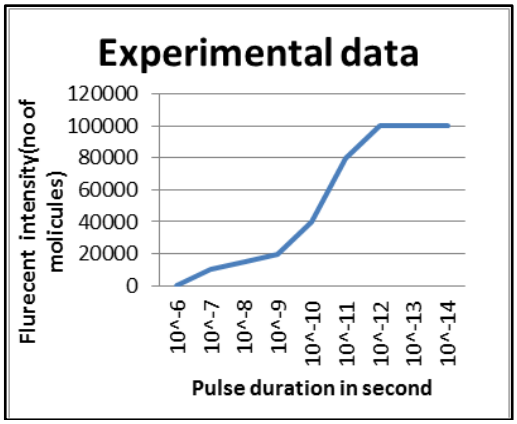

Figure 5. Microscopic real-time image of a typical osteoblast cell undergoing PI uptake

The effects of picosecond electrical pulses on the intra organelle are also demonstrated by the uptake of dyes and the orientation of phosphatidylserine in the membrane after applying pulses. Three of the dyes most often used to study changes in plasma membrane permeability are trypan blue, propidium iodide (PI), and ethidium homodimer. The above figure shows the uptake of PI by osteoblast cells. It is interesting that the increase in fluorescence is observed only after approximately 12 minutes and then completed in one minute. This indicates that the formation of pores large enough to allow passage of propidium iodide is a secondary effect, following the formation of nanopores, which occurs on a picosecond timescale. It is likely that the nanopores are too small to allow PI uptake immediately and the secondary PI uptake is due to rapture of intra organelle.

4.6 Observations

(a) (b)

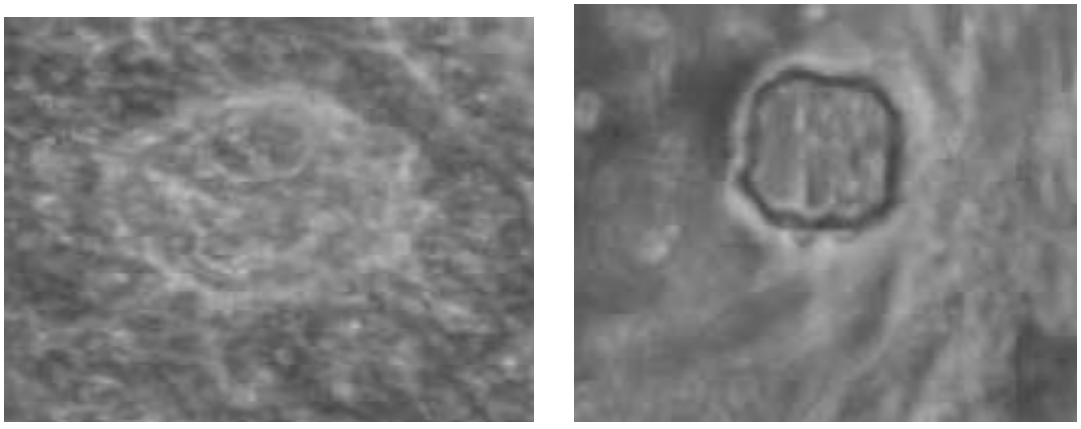

Figure 6. Morphological views of intra organelle Nano Poration of osteoblast cell in 3D hybrid microchip: (a) before intra organelle nano poration; (b) after intra organelle pico poration

Above figure shows the morphological changes of osteoblast cell. In Figure 6(a) dense osteo cell. When the micro pulse is applied the cell starts to response but it is unable to

penetrate the cell membrane which is exposed in fig 6(b), expected results will come when we apply the Pico pulse on the cell, a number of nano pores are generated on the intra organelle and chemicals are entered into the cell, that shows in the figure .From this observation it is exposed that there is no effect of micro pulse but pico pulse penetrate the on intraorganelle .It supports the numerical and analytical result explore in this research. .It supports the numerical and analytical result explore in this research.

4.7 Application of neuro fuzzy network for image reorganization of intra organelle nanoporation

The image after ion uptake of intra organelle under the influences of pico pulse in proposed hybrid micro chip, can easily analysis by neuro-fuzzy algorithm to explain the proper phenomenon of nanoporation. In this context we use adaptive resonance algorithm which is explain as follows

Step 1: Select the first input as the leader or representative of the first cluster.

Step 2: classify all the input vectors using present neural network.

Step 3: Search for the most poorly classified input vector.

Step 4: IF the selected input vector has a similarity degree lower than a threshold, THAN create a new cluster with the selected input vector as a leader and go to step 2, ELSE stop the process.

The graphical reorganization of the nanoporative image as follows

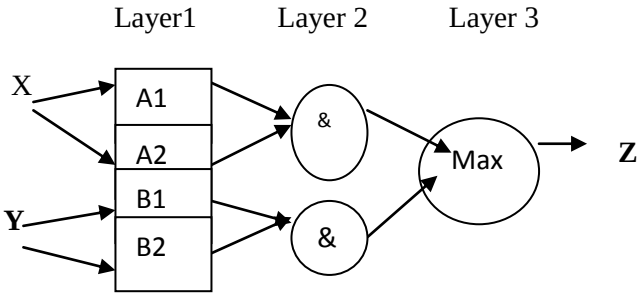

Rule 1: IF x is A_1 and y is B_1, THAN z1=fired strength$\omega 1$.
Rule 2: IF x is A_2 and y is B_2, THAN z_2=fired strength $\omega 2$.

To recognize the image of the nanopores the following mechanism is adapt.

Step 1: Rule constriction.

Step 2: Verification of leader.

Step 3: Training membership function.

Step 4: Verification of classification quantity.

Step 5: IF the leader do not correspond THAN add rules and possibly membership function to avoid the misclassification.

Step 6: Achieve fine tuning of the system by optimized all membership function.

Step 7: IF the slice image has not been reached THAN go to step 2, ELSE stop.

By using this ALGORAM, the image of intra organelle nanoporation obtain from simulation can easily be recognized and images are as fig.9.

5. Results and Discussion

This part of our study dedicated to Numerical simulation of intraorganelle nanoporation in the intrigrated 3D hybrid microchip and the synchronization among the COMSOL simulation, MATLAB numerical analysis and experimental observation. As we already explore the COMSOL simulation and experimental observations so remaining contribution are completed through the graphical representation of various parameters intraorganelle nanoporation through MATLAB simulations. This part evaluate different factors of the intra organelle nanoporation of a dense osteoblast cell located in the micro chip of height (500μm), cell of radius a (12μm), electrodes of width (50μm).in a different pico pulse intensity**.**

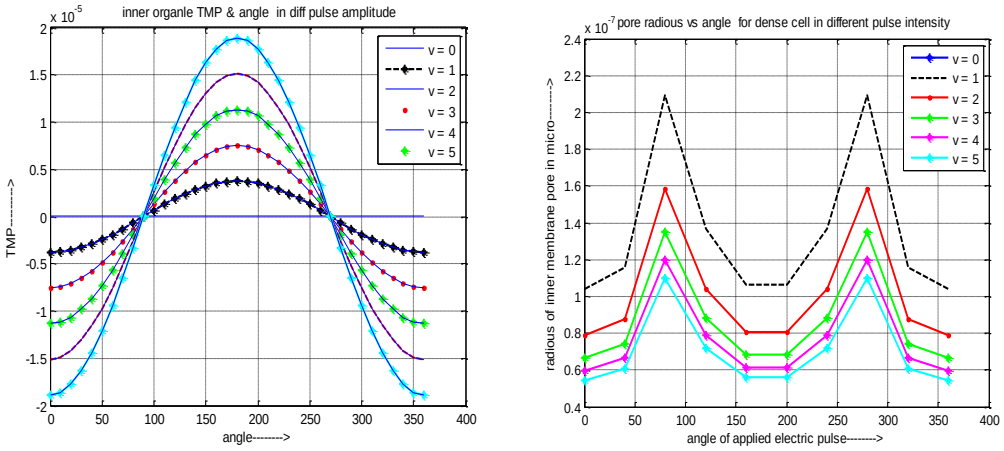

Figure 7(a). Pulse evaluation of the intra organelle membrane potential; 7(b). Pulse evaluation of the intra organelle pore radius

Figure 7(a) shows the intra organelle potential of dense osteoblast cell. For inner organelle we get the response only when the pulse intensity & width are in above pecoscale range. It is exposed that pores are formed only when the pulse duration is in Pico second range and the intra organelle potential is gradually decrease until the nanopores are generated and once the nanopores are generated, the TMP increase. The TMP has a sharper decrement at the poles (θ=0 & θ= *360*).The value of TMP independent of pulse duration, directly proportional pulse interval but inversely proportional with pulse intensity. As the nanopores are created, TMP increases and the angular positions of the highest TMP and the biggest nanopores move just opposite to the equator (E). In the case intra organelle potential is gradually increase until the nanopores are generated and once the nanopores are generated, the potential is reduced. It has a sharper reduction at the poles (θ= *180*) and its value directly proportional with value of pulse duration and intensity but inversely proportional with pulse interval. As the nanopores are created, intra organelle potential decreases and the angular positions of the highest voltage and the biggest nanopores move toward the equator (E). In all cases no voltage is obtain at the pole θ=90 & θ= *270* and negative TMP is exposed during poles θ=0 to 89 & θ=271 to 3*60* due to the effect of rest potential. We also find out that the curve analysis of cytoplasm and nucleus are opposite in nature which reflects their reverse dielectric property and applied

pulse nature provides the new information about the window effects in intra organelle of the rigid cell.

The Figure 7(b) explores the variation of intra organelle pore radius along with pole position of applied electric field. It clears that the radius of all the pores are not same it is sinusoidal distributed over the whole surface of nucleus. The value of the pore lies in between 60 to 200 nano meter. The biggest nano pores are generated at pole θ=90 and *270,* where we get the maximum potential.as the nanopores are created, intra organelle potential increases and the biggest nanopores move just opposite to the equator (E). It is also shown that the location of the pores are as same as outer membrane and pore radius is gradually increase as the angle of applied electric field is increase & maximum pore radius is obtain at an angle of θ= *90* after that it starts decrease. We also find out that the pore radius of outer membrane is greater than the radius of inner membrane of the organelle due to the higher elasticity of layers.

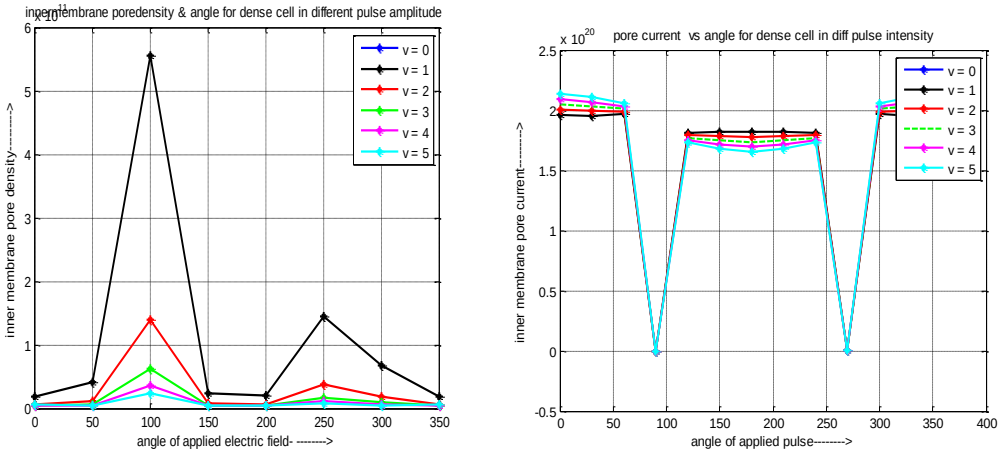

Figure 7(c) Pulse evaluation of the inner pore density; 7(d) Pulse evaluation of the inner membrane pore current of a single osteoblast

Figure 7(c) depicts the variation of intra organelle pore density of multilayer dense osteoblast cell. In case of pore density the pulse specifications have an acceptable effect although the maximum pore density locate at the pole (θ=*100 & 250*) which is independent of above variations. The effectiveness of pulse specification on inner membrane pore density is same as outer membrane but the value of pore density of inner membrane is low compare to outer membrane of the organelle. This information reflects that the outer membrane is more permeable than inner membrane but maximum pore density lies in the same pole (θ= *100 & 250*) for both layers.We also find that in inner membrane pore density is inversely related to each another. For drug delivery system we need maximum pore density region which is exposed through this numerical analysis. Figure 7(d) shows the variation of intra organelle pore current provided on membrane for dense osteoblast cell. In this respect we get the response only when the pulse intensity & width are in above picoscale range and the minimum pore current at pole θ= *90 & 270* where organelle potential is also minimum but biggest nanopores are generated. We find out that the curve analysis the value of outer membrane pore current is lower than inner membrane of the organelle having the same specification. It reflects the different molecular structure of outer & inner part of the organelle.

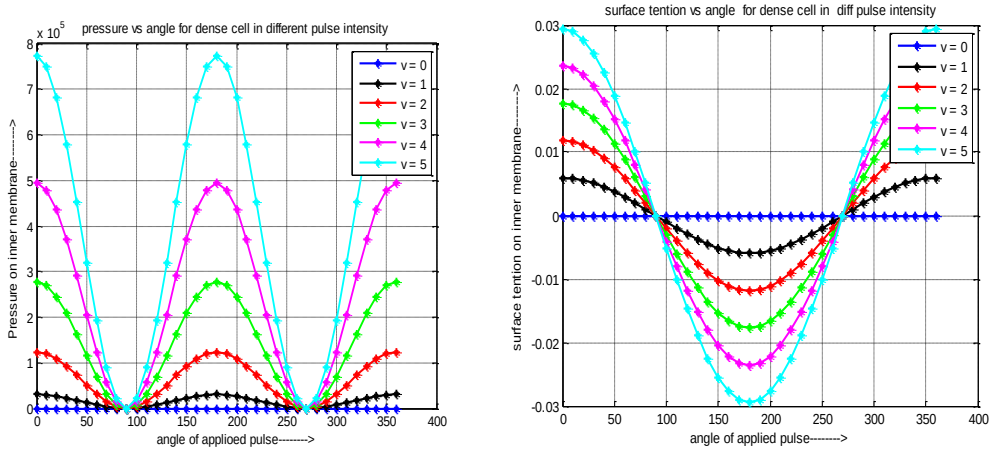

Figure 7(e). Pulse evaluation of the intra organelle pressure; 7(f). Pulse evaluation of the intra organelle surface tension of a osteoblast

In Figure 7(e) the variation of pressure provided on intra organelle of dense osteoblast cell is exposed. For intra organelle we get the response only Pico second pulse. It is also exposed that pressure is directly link with intra organelle current and both non uniformly distributed over the whole surface of the organelle. There the minimum value is exposed at pole $\theta = 90 \& 270$ which is independent of pulse, electrode, micro channel and suspension media specification. We find out that the curve analyses of outer membrane pressure are lower than inner membrane of the organelle, having the same specification. It reflects the different molecular structure of outer & inner membrane part of the organelle. Figure 6(f), depicts the variation of outer membrane surface tension for single and dense osteoblast cell. In all cases the surface tension is varied in cosine form change in pole in between electric field and radius vector. In every conditions the zero surface tension is obtained at pole ($\theta = 90 \& 270$) which assigned the minimum pressure and maximum pore radius at that pole, although value of surface tension is directly proportional with pulse duration and intensity but inversely proportional for pulse interval. As we know the critical voltage of a membrane potential is control by surface tension so if the surface tension is changed than the critical voltage is also non uniformly distributed over the membrane which assigned the different radius of the pore which is generated in the membrane for unique external electric field? Practically for efficient electroporation we need minimum surface tension which may cause the maximum pore density on the membrane. For dense cell where positive surface tension exposed from pole $\theta = 91$ to 269 and value is directly varied with pulse width and it should be minimum for efficient electroporations. We also find out the negative surface tension region in the remaining part of the membrane except $\theta = 0$ and 270, which implies that such part of membrane will inherently have an inverse Kelvin vapor pressure effect, that resulting in increased water condensation. For single or dense cell the nature of the curve is same but in dense cell value of surface tension is lower as compare to single cell which indicates the rigidity of the previous cell.

6. Conclusion

In this paper represents the effect of pico electric field on intra organelle nanoporations under the influences of the smart controlled FPGA based pico second pulse on. It is observed that When the micro pulse is applied the cell starts to response but it is unable to penetrate the

cell membrane where as the expected results will come when we apply the Pico pulse on the cell, a number of Nano pores are generated on the intra organelle and chemicals are entered into the cell.After completion of study It is exposed that pores are formed only when the pulse duration is in Pico second range and the intra organelle potential is gradually decrease until the nanopores are generated and once the nanopores are generated, the TMP increase. The TMP has a sharper decrement at the poles ($\theta = 0$ & $\theta = 360$). When the value of TMP reaches the critical value it may cause the generation of nano pores. It clears that the radius of all the pores are not same and it is sinusoidal distributed over the whole surface of nucleus. The value of the pore lies in between 60 to 200 nano meter. The biggest nano pores are generated at pole θ=90 and 270, where we get the maximum potential. For pore current we get the response only when the pulse intensity & width are in above Pico scale range and the minimum pore current at pole θ= *90 & 270* where organelle potential is also minimum but biggest nanopores are generated. It is also exposed that pressure is directly link with intra organelle current and both non uniformly distributed over the whole surface of the organelle. There the minimum value is exposed at pole θ= *90 & 270* which is independent of pulse, electrode, micro channel and suspension media specification. We also study this property and in all cases the surface tension is varied in cosine form change in pole in between electric field and radius vector. In every conditions the zero surface tension is obtained at pole (θ= *90 & 270*) which assigned the minimum pressure and maximum pore radius at that pole, although value of surface tension is directly proportional with pulse duration and intensity but inversely proportional for pulse interval. On the other hand we also find out that ,in case of pore density the pulse specifications have an acceptable effect although the maximum pore density locate at the pole (θ= *100 & 250*) which is independent of above variations. As we know the pore density of the organelle has great influences on ion uptake and in our study it is explored that the amount of ion which is uptake by the intra organelle is only occurred at Pico scale pulse and its value is not same throughout the whole surface of the layer of the nucleus. It is changed sinusoidal in nature over the surface. The maximum ion uptake occur at pole θ=*0 & 360* and zero value exposed at pole (θ= *100 & 250*) where the surface tension is minimum. As a whole the complete nanoporation of intra organelle is characterized in our study and finally this numerical model also supports the faithful pattern reorganization of biological cell image after intra organelle nanoporation using neural fuzzy network which is first time implement for nanoporation .All these are related to the dielectric, elect kinetic properties of multilayer dense osteoblast cell which can also aid in understanding the basic physiological difference between normal and cancerous bone cells on a molecular level and finally all the information given in this article might provide a new light on drug delivery system and cancer treatment in bone cell. We are in process and more work has to be done to explore these possibilities.

Acknowledgements

All of we wish to thank Dr. Soumen Das (IIT, KGP) for assistance with analytical data processing throughout the whole work.

References

[1] M. y. Esmail, L. Sun, L. Yu, H. Xu and L. Shi, "Effects of PEMF and glucocorticoids on proliferation and differentiation of osteoblasts Electromagn", Biol Medvol., vol. 31, **(2012)**, pp. 375–381.
[2] G. S. Stein and J. B. Lian, "Molecular mechanisms mediating proliferation/differentiation interrelationships during progressive development of the osteoblast phenotype", Endocr Rev., vol. 14, (**1993**), pp. 424–442.

[3] M. De Mattei, A. Caruso, G. C. Traina, F. Pezzetti and T. Baroni, "Correlation between pulsed electromagnetic fields exposure time and cell proliferation increase in human osteosarcoma cell lines and human normal osteoblast cells in vitro", Bio electromagnetic, vol. 20, **(1999),** pp. 177–182.
[4] C. H. Lohmann, Z. Schwartz, Y. Liu, H. Guerkov and D. D. Dean, "Pulsed electromagnetic field stimulation of MG63 osteoblast-like cells affects differentiation and local factor production", Orthop Res., vol. 18, **(2000),** pp. 637–646.
[5] Y. Wei, H. Xiaolin and S. Tao, "Effects of extremely low-frequency-pulsed electromagnetic field on different-derived osteoblast-like cells", Electromagn Biol Med., vol. 27, **(2008),** pp. 298–311.
[6] M. Hartig, U. Joos and H. P. Wiesmann, "Capacitively coupled electric fields accelerate proliferation of osteoblast-like primary cells and increase bone extracellular matrix formation in vitro", Eur Biophys., vol. 29, **(2000),** pp. 499–506.
[7] Y. Yamamoto, Y. Ohsaki, T. Goto, A. Nakasima and T. Iijima, "Effects of static magnetic fields on bone formation in rat osteoblast cultures", J Dent Res., vol. 82, **(2003),** pp. 962–966.
[8] G. Scott and J. B. King, "A prospective, double-blind trial of electrical capacitive coupling in the treatment of non-union of long bones", J Bone Joint Surg Am., vol. 76, **(1994)**, pp. 820–826.
[9] P. Ellappan and R. Sundararajan, "A simulation study of the electrical model of a biological cell", Journal of Electrostatics, vol. 63, **(2005),** pp. 297-307.
[10] I. Meny, N. Burais, F. Buret and L. Nicolas, "Finite-Element Modeling of Cell Exposed to Harmonic and Transient Electric Fields", IEEE transactions on magnetic, vol. 43, **(2007),** pp. 654-660.
[11] C. Yao, X. Hu, Y. Mi, C. Li and C. Sun, "Window Effect of Pulsed Electric Field on Biological Cells", IEEE Transactions on Dielectrics and Electrical Insulation, vol. 16, no. 5, **(2009),** pp. 1323-1326.
[12] S. Sarkar, "3D Microelectrode Geometry Effects the Multilayer Dense Osteo Intra-organelle Membrane Potential Characterization", International journal of computer application, vol. 80, **(2013),** pp. 17-25.
[13] S. Sarkar, "A Theoretical Study of Bi-Layer Osteoblast Cell Electroporation in a Micro Channel at Radio Frequency", Journal of Biomaterials and Tissue Engineering, vol. 3, **(2013),** pp. 1-19.
[14] S. Sarkar, "Study the Window Effect of Rectangular Electrical Pulse in Membrane Potential of Dielectric Model of Osteoblast Cell under Different Microelectrodes", International Journal of Engineering Research and Development e-ISSN: 2278-067X, p-ISSN: 2278-800X, www.ijerd.com, vol. 5, Issue 9, **(2013),** pp. 22-29.
[15] S. Sarkar, "Characterization of dense osteoblast pore current in a 3d microchip", International Journal of Electrical and Electronics Engineering Research (IJEEER) ISSN 2250-155X, vol. 3, Issue 4, **(2013),** pp. 51-60.
[16] S. Sarkar, "Analysis of Dense Osteoblast Surface Tension in a Micro Chip", International Journal of Engineering Research and Development, vol. 8, issue7, **(2013),** pp. 98-112.
[17] S. Sarkar, "Characterization of Intra organelle Nanoporation of Multilayer Dense Osteoblast cell", International journal of computer application, vol. 83, **(2013),** pp. 15-22.
[18] W. Krassowska and P. D. Filev, "Modeling Electroporation in a Single Cell", Biophysical Journal, vol. 92, **(2007),** pp. 404–417.
[19] S. Talele and P. Gaynor, "Non-linear time domain model of electropermeabilization: Response of a single cell to an arbitrary applied electric field", Journal of Electrostatics, vol. 65, **(2007),** pp. 775–784.
[20] M. B. Fox, D. C. Esveld, A. Valero, R. Luttge, H. C. Mastwijk, P. V. Bartels, A. Van Den Berg and R. M. Boom", Electroporation of cells in microfluidic devices: a review", Anal Bioanal Chem., vol. 385, **(2006),** pp. 474–485.
[21] K. A. DeBruin and W. Krassowska, "Modeling Electroporation in a Single Cell. II. Effects of Ionic Concentrations", Biophysical Journal, vol. 77, **(1999),** pp. 1225–1233.
[22] X. Zhao, M. Zhang and R. Yang, "Control of pore radius regulation for electroporation-based drug delivery", Commun Nonlinear Sci., vol. 15, **(2010),** pp. 1400–1407.

